IOSR Journal of Applied Geology and Geophysics (IOSR-JAGG)
e-ISSN: 2321–0990, p-ISSN: 2321–0982.Volume 11, Issue 5 Ser. I (Sept. – October. 2023), 49-63
www.iosrjournals.org

Hydrogeological Analysis In The Surroundings Of The Camaçari-BA Landfill Using The Electrical Geophysical Method

Cleber de Jesus Santos[1]
[1](*Institute of Geosciences/ State University of Campinas, Brazil)*

Abstract:
Background*: The lack of knowledge about aquifer recharge zones has caused serious problems related to their preservation, for example the contamination of aquifers in urban areas by industrial establishments and residences. This context has motivated numerous studies aimed at mapping aquifers and monitoring their degree of preservation. To this end, geophysics is a promising tool given its ability to comprehensively investigate the subsurface without the need for drilling, a risky procedure that increases the risk of contamination, especially in landfill areas.*
Materials and Methods*: This work consist in use of IP-Resistivity surveys for hydrogeological characterization in the area of the Jardim Limoeiro, Camaçari-Bahia. Six Vertical Electrical Sounding (VES) were executed in the study area, and used 15 others by the Centro de Pesquisa em Geologia e Geofisica (CPGG) of the Universidade Federal da Bahia. The surveys were carried out with the Schlumberger array with maximum electrode spacing AB/2 up to 300m. All surveys used in this study were inverted unidimensionaly and later were interpreted with the aid of geological and geophysical logs of nearby wells.*
Results*: It was possible to map the subsurface in the study area up to 80m deep. In the final geoelectrical model is possible to identify the position of the partially saturating Formation Marizal static level; to estimate the transition zone of Formation Marizal to Formation San Sebastian, and infer the presence of sandstone saturated with water, bounded by clays.*
Conclusion: *The methodological strategy adopted was able to efficiently identify and distinguish areas associated with soil contamination at the shallowest depths in the central area of the landfill. The ability to identify plumes of contamination and also verify the integrity of the soil sealing blankets attests to the efficiency of the method adopted for landfill management.*
Key Word*: Geophysics; Contamination of Aquifers; Formation San Sebastian; Vertical Electrical Sounding*

Date of Submission: 20-09-2023 Date of Acceptance: 30-09-2023

I. Introduction

The continuous increase in the cost of treating water for human consumption has prompted numerous studies to identify underground water reserves. Electrical geophysics research has made a significant contribution to this scenario, as its ability to image the subsurface is safe, versatile and inexpensive. Geoelectrical prospecting methods have been used all over the world with great success in hydrogeological characterization, both because of the safety and accuracy of the results obtained.

The aim of this study is to apply the IP-resistivity method to hydrogeological characterization in Jardim Limoeiro, located in the municipality of Camaçari, in the State of Bahia. The curves from vertical electrical soundings were used to identify geological features containing water, the boundaries between the saturated and unsaturated zones and even to infer considerable lithological changes. This work contributes to expanding hydrogeological knowledge of the area, as well as serving as a source for future research, since there is little work of this nature carried out in the area under study.

The methodology used consists of gathering bibliographic information, selecting available well profiles in the area and surveying surface geological information. Vertical electrical IP-Resistivity surveys were carried out using the Schlumberger electrode array between 18/10/2011 and 22/10/2011, to which other SEVs made available by the Geology and Geophysics Research Center (CPGG UFBA) were added. The soundings were processed using the IPI2win program and interpreted together with the geological and geophysical profiles of the wells, resulting in a geoelectric model of the study area.

The work is organized into four chapters: Geology and Hydrogeology of the Study Area; Theoretical Framework of Electrical Methods; Data Acquisition, Processing and Interpretation;

II. Material And Methods

General Characteristics

The area investigated is located in the eastern industrial sector of the Camaçari petrochemical complex (UTM coordinates 8596000 and 8599000 south latitude and 586000 and 578000 west longitude, DATUM - SAD 69/Zone 24). Located in Loteamento Espaço Alfa, Jardim Limoeiro, Camaçari-BA (Figura 1). More precisely, the stretch of Via Atlântica that connects the Continental Pneus company to CETREL. This area is home to the Camaçari Landfill, where most of the surveys were carried out.

Figura 1: Localização da área de estudo com destaque para os pontos de coleta.

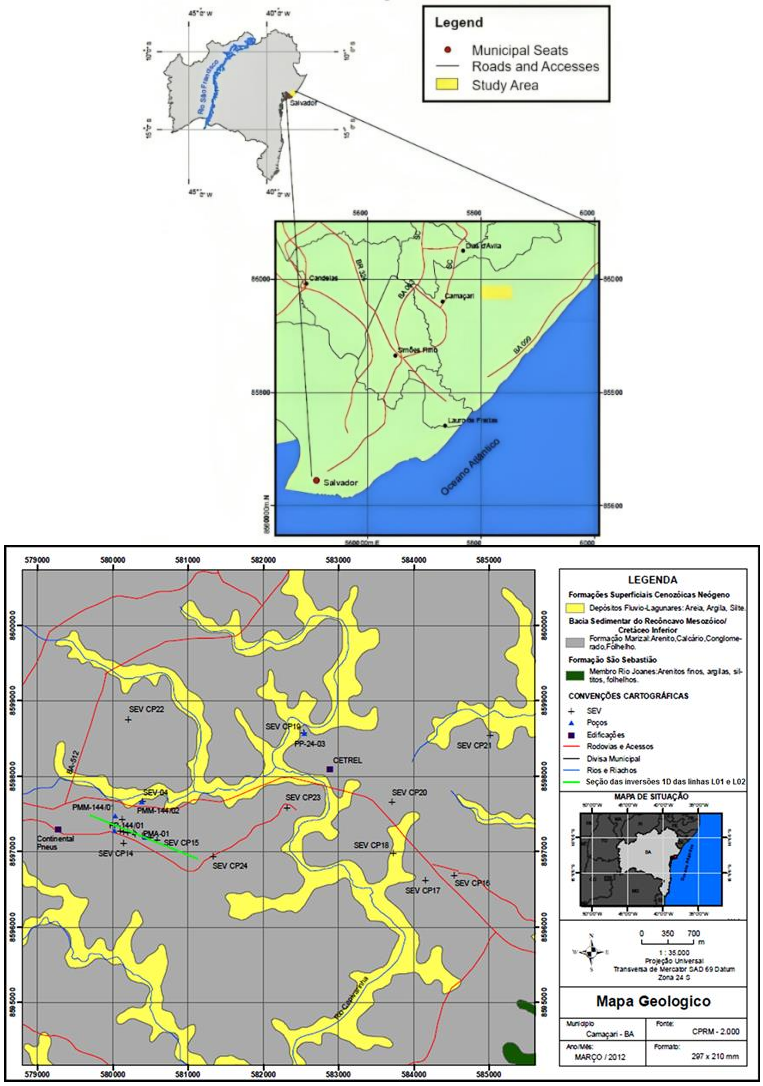

Source: author's own.

According to the Koppen classification (Af), the region's climate is hot and humid, typical of a tropical region near the coast, with the period between September and February being dry, with sporadic rainfall, and with rainfall concentrated between April and August. The average annual temperature is 24.5 C, with total rainfall averaging 1,823 mm per year and 250 mm per month (WATERLOO, 2003).

Geomorphologically, the area is characterized by a uniform plain composed of sediments, with small coastal elevations and tablelands, with altitudes varying between 60 and 200 metres (WARMING, 1981). The vegetation present in the region is basically secondary, since the original was practically destroyed and only a few scattered specimens remain. This vegetation is made up of low, scattered shrubs on grasses; ombrophilous forest, often replaced by reforestation trees; and scattered patches of forest (FONSECA, 2004). The soils found in the region are of the type Latossolos Argilosos, Espodossolos Quart zarênicos and Argissolos, according to studies carried out by Embrapa (CNPS, 2006). As can be seen in figure 1, the area under investigation contains sediments of the São Sebastião and Marizal formations, as well as Cenozoic coverings represented by the Barreiras Group and superficial formations.

The regional context of the environment studied is the result of crustal stretching that gave rise to the Recôncavo intra-continental rift. This, in its evolutionary process, was subject to intense tectonic activity followed by high rates of subsidence and later high rates of sedimentation filling the depocenters, the largest of which is known as the Baixo de Camaçari, located in the municipality where the study was carried out. The area studied is located in the northern compartment of the Recâncavo Basin, Bahia-Brazil. The Recôncavo Basin is an integral part of the Recôncavo-Tucano-Jatobá system, an aborted intra-continental rift, implanted in the current coastal region of northeastern Brazil and which preceded the initial stages of the opening of the Atlantic Ocean, during the Eocretaceous, due to the crustal stretching processes that led to the fragmentation of the Gondwana supercontinent (MAGNAVITA et al., 2005; SZATMARI et al., 1984).

Electrical Method

Electrical geophysical prospecting methods use the electrical parameters of soils and rocks, such as resistivity or electrical conductivity, spontaneous potential and polarisation, to investigate subsurface geology, as stated by Ward. Based on measuring the potential difference between two regularly spaced electrodes, the electrical resistivity method identifies physical parameters such as resistivity, spontaneous potential and induced polarisation of the different materials in the subsurface. This occurs due to the injection of a continuous or very low frequency electric current into the crust. The theory of electricity and electromagnetism are the domains that underpin the theory of this method (WARD, 1990). The electrical resistivity method stands out for being non-invasive. This is important in cases involving groundwater contamination, as it is cheaper than methods that use monitoring wells and is subject to less noise than other geophysical methods.

The propagation of electric current in a rock body can basically take place in two ways: firstly through the transport of electrons in the rock matrix (metallic minerals, impurities and mineral aggregation) and secondly through the displacement of ions dissolved in the fluid contained in the pores and fissures of rocks and soils. Each rock has a wide range of variability in its own resistivity values (Figure 2), which depend on the degree of homogeneity, the levels of alteration, the degree of rupture of the rocks, their primary porosity, as well as their saturation and clay content. In the case of unconsolidated soils, such as recent alluvial deposits, resistivity depends on grain size, the fluids contained in them and the content of salts dispersed in them. The exception to this rule is clays which, even when compacted, have extremely low resistivity values; this phenomenon is mainly due to the characteristics of the crystalline reticulum of the minerals that make them up and their degree of saturation.

Figure 2: Resistivity and electrical conductivity of some minerals and rocks.

Materiais	Resistividade (Ω .m)	Condutividade (mS/m)
Granito(úmidos e seco)	$4,5.10^3 - 1,3.10^6$	$0,0008 - 0,22$
Gabro	$10^3 - 10^6$	$0,001 - 1$
Xisto	$20 - 10^4$	$0,1 - 50$
Mármore	$100 - 2,5.10^8$	$0,000004 - 10$
Quartzito	$10 - 2.10^8$	$0,000005 - 100$
Argilito	$10 - 800$	$1,25 - 100$
Calcário	$50 - 10^7$	$0,0000001 - 20$
Argila(úmida e seca)	$1 - 100$	$10 - 1000$
Areia(úmida e seca)	$1 - 10^4$	$0,1 - 1000$
Água doce(20^oC)	80	12,5
Água Subterrânea	$0,5 - 300$	$3,3 - 2000$
Água do Mar	0,2	5000
Solo	$1 - 10$	$100 - 1000$

Source: Telford (1990)

According to (WARD, 1990), for a point source injecting a current of intensity I into the interior of a homogeneous and isotropic conducting half-space of resistivity, representing a flat Earth, the electric potential at an observation point P, located at a distance r from the source electrode, is given by:

$$V(r) = \frac{I.\rho}{2\pi.r}$$

Since the potential function is a scalar quantity, the total potential due to various sources can be obtained by adding the contributions of each source considered separately. Applying this principle to the quadrupole, the potential difference between points M and N, generated by injecting currents at points A and B, is given by:

$$\Delta V = \frac{I.\rho}{2\pi}\left(\frac{1}{AM} - \frac{1}{BM} - \frac{1}{AN} + \frac{1}{BN}\right)$$

ou ainda:

$$\rho = k\,\frac{\Delta V}{I}$$

Onde,

$$k = 2\pi\left(\frac{1}{AM} - \frac{1}{BM} - \frac{1}{AN} + \frac{1}{BN}\right)^{-1}$$

It is referred to as the geometric factor of the arrangement because it depends solely on the relative arrangement of the electrodes in the terrain. The equation above is used to calculate the resistivity of a homogeneous and isotropic medium. However, in practice, due to the heterogeneous nature of the rock, the subsurface cannot be considered a homogeneous medium. Therefore, the measured quantity represents the resistivity that the medium would have if it were homogeneous, which is why the found resistivity is termed apparent. This parameter represents the result of measurements in some of the geoelectric methods (Braga, 2006). For heterogeneous and/or anisotropic mediums, the resistivity calculated in this way will vary with the position and/or orientation of the electrode arrangement (MOTA, 2004).

Vertical Electrical Sounding (VES)

The Vertical Electrical Sounding (VES) technique involves the vertical and pointwise analysis of the subsurface based on a series of measurements of physical parameters (resistivity and/or chargeability) taken from the surface. Mathematically, this technique analyzes and interprets the function known as apparent resistivity. For the development of this technique, we utilize the Schlumberger electrode arrangement.

Widely used for its convenience in data acquisition procedures, data quality, and safety, the Schlumberger electrode arrangement is established by setting up a circuit on the ground with four electrodes, including two current electrodes and two potential electrodes placed between them. All electrodes are spaced relative to the center of the sounding.

In this arrangement (Figure 3), the sounding is conducted by increasing the separation (2a) between the current electrodes while keeping the potential electrodes fixed at separation (b), until the instrumental precision limit of the system used is reached. As it is generally not possible to perform the entire sounding with a single MN setup due to the diminishing received signal (field measurement) and consequent loss of reading precision, the resistivity measurement is repeated at certain points with two MN values (recovery readings) for the same AB/2 value. This procedure allows for the detection and sometimes correction of surface heterogeneity effects that occur when MN positions are swapped (KIRSCH and YARAMANCI, 2006). The geometric coefficient of the Schlumberger arrangement is given by the following expression.

$$k = \pi\left(\frac{a^2}{b} - \frac{b}{4}\right)$$

Figura 3: Arrangement of electrodes for the Schlumberger setup.

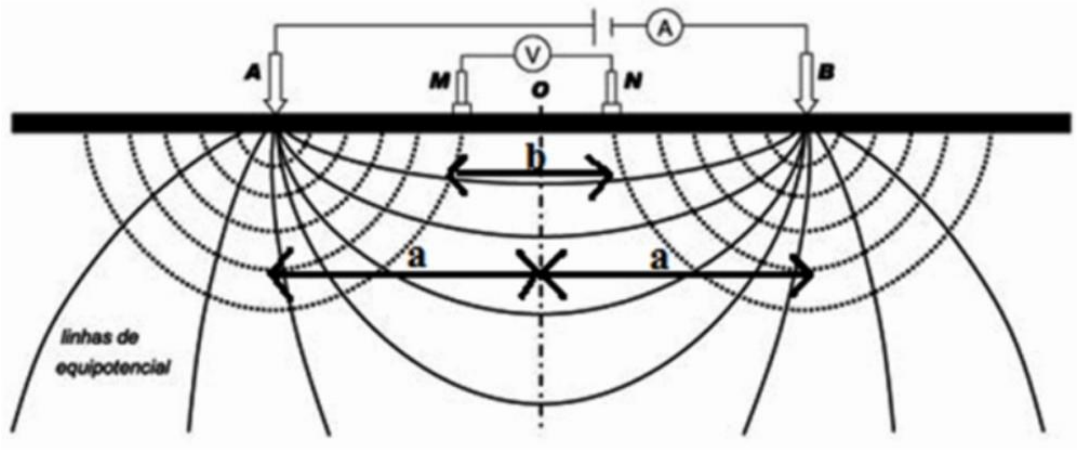

Source: Adapted from Braga (2006).

Datta Collection

The resistivity and apparent induced polarization data obtained during the surveys were acquired using the Syscal Pro apparatus, a 10 channel system, manufactured by Iris Instruments (Figure 4). The apparatus is

equipped with an internal 12V battery coupled with a DC-DC converter that operates on direct current and can produce a maximum output voltage of 800V. This same apparatus simultaneously measures electrical resistivity, spontaneous potential, and apparent induced polarization in the time domain. It also performs spontaneous potential compensation and reduces natural or artificial noise through current polarity reversals.

Figure 4: Sycal Pro – 10 channels.

Source: author's own.

The data recorded by the apparatus were immediately documented and plotted on the bilogarithmic chart contained in the field worksheet. This chart includes interpolated sounding points and provides a preliminary view of resistivity behavior at that specific location. In addition to the apparent resistivity data, the recorded values of potential difference (ΔV), electric current intensity (I), and apparent chargeability (Ma) constituted crucial information for data quality control.

During the geophysical data acquisition process, a comprehensive geological study of the area was conducted (Figure 5). We had access to well data in addition to information obtained from surface mapping, geological maps, satellite imagery, geo-electric (ER, DIR) and radiometric (Gamma) profiles. This information was essential for geophysical acquisition, especially in accurately positioning the sounding points.

In the planning phase for data acquisition, the locations of the sounding centers, their expansion directions, and the spacings to be used were established. These spacings were previously marked with adhesive tapes to streamline the acquisition process. The maximum spacing of 300m for AB/2 values was determined based on site visits, geological map analysis, and satellite images obtained from Google Earth.

The distance between the centers of the soundings within the landfill was established to provide a satisfactory correlation between them since data arrangement and electrode opening direction vary according to the acquisition objectives. This description effectively captures the behavior of physical parameters in the subsurface with quality and safety.

Functionality tests of the equipment were conducted, GPS configurations were set, cable tests were performed, and the condition and insulation of the wiring and clamps were verified. These procedures were executed to prevent current leakage during field acquisition and ensure the quality and accuracy of the acquired data. Care was also taken to maintain symmetry in the opening of the current and potential electrodes relative to the sounding center, so that the apparatus provided measurements with equal and fixed spacings.

It was considered in the planning that the spacing between the current electrodes, relative to the potential electrodes, should respect the precision limit of the instrument used. Therefore, it was not possible to have the same MN spacing for all AB/2 measurements due to the decrease in the measured signal in the field. As a procedure, two measurements with two MN values were taken while keeping the same AB/2 measurement. This procedure, known as recovery reading, aims to correct the effects of surface heterogeneities that occur when MN positions are swapped.

In the field, copper metal bar electrodes were used. They were buried in the soil and connected by a system of conductive cables. Contact resistances between the electrodes and the soil were reduced, increasing the contact area between them. However, sometimes it was necessary to wet them with saltwater. Regarding contact resistance issues, the high rainfall levels recorded during the acquisition period greatly facilitated the execution of the work.

Figura 5: Simplified Geological Map of the studied area, with emphasis on the Camaçari Landfill.

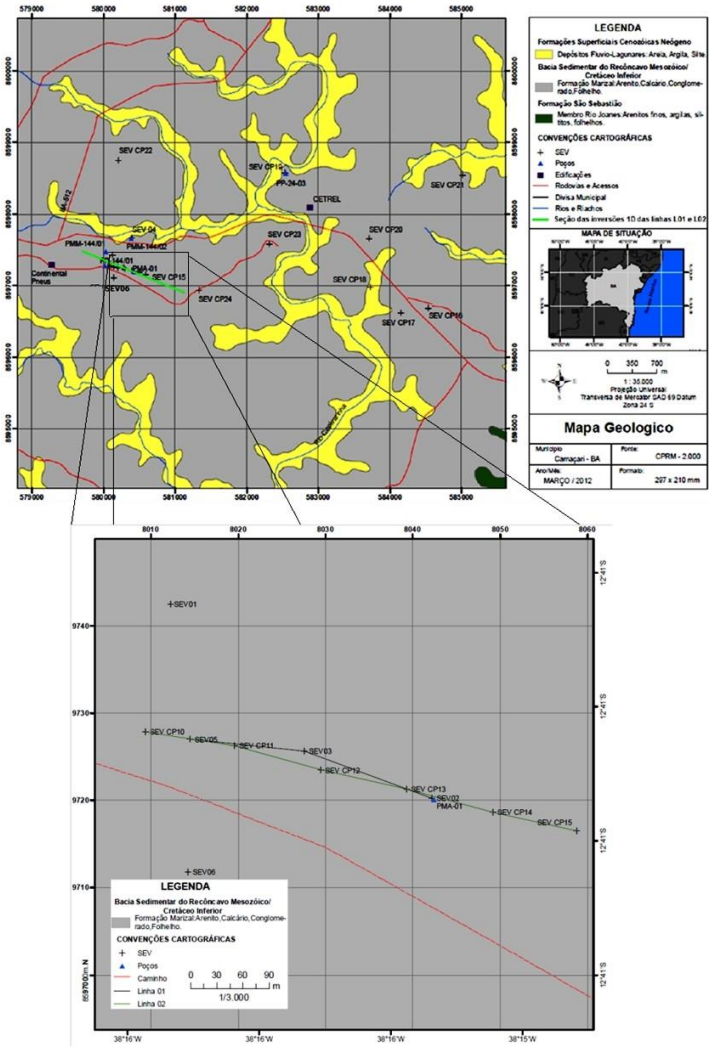

Source: Created by the author.

The VES01 was conducted over the oldest cell of the Sanitary Landfill. Its purpose is to assess the resistivity behavior in an area of solid waste disposal, for later comparisons with data obtained from more distant locations (Figures 6)

Figure 6: Survey Layout in the Camaçari Sanitary Landfill Area.

Source: Created by the author.

III. Result

Given the set of data available, it is possible to successfully obtain a qualitative overview of the saturated and unsaturated domains. This characterization is based on a total of 21 VES (Vertical Electrical Sounding) surveys, of which 6 were conducted exclusively for this study, in association with well profiles available in the study area.

The purpose of these surveys is to determine the spatial distribution of physical parameters in the subsurface, starting from point data observed at the surface of the terrain. They also seek the geological significance of these parameters. When used in conjunction with profile information, whether geological or geophysical, they allow for a consistent characterization of significant lithological changes.

It is possible to distinguish geoelectric strata between sandy sediments and clayey sediments and, among other things, water-saturated zones (Figure 7).

Figure 7: Representative electrical sounding curves. (A) SEV05, SEV06, SEV03, SEV02. (B) SEVCP20, SEVCP18, SEVCP17, SEVCP16.

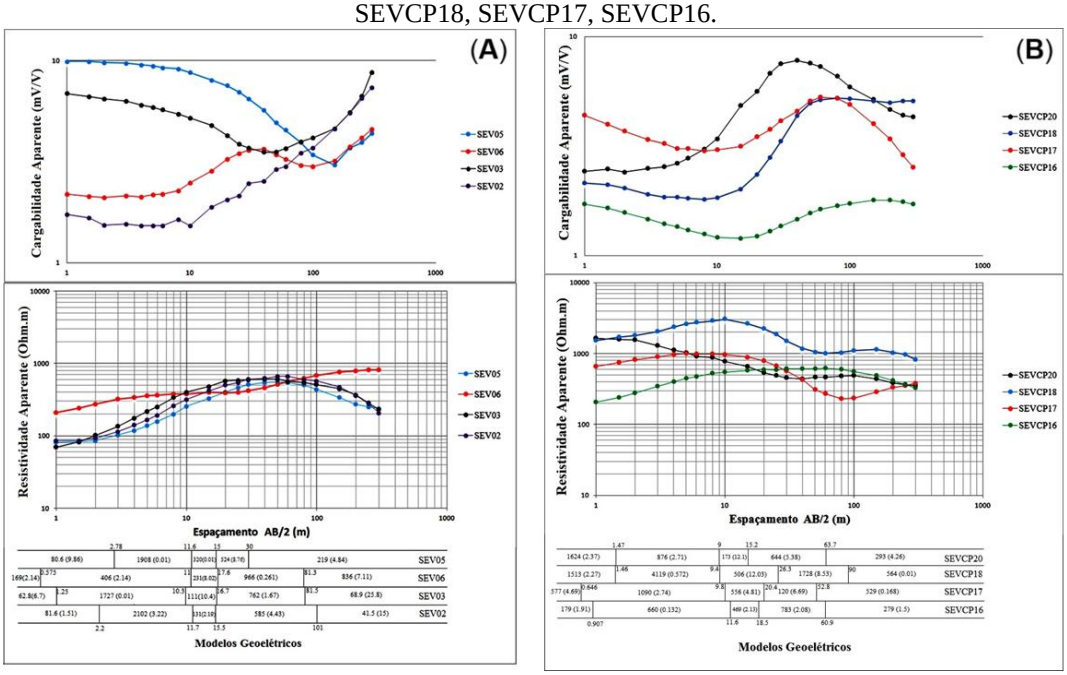

Source: Created by the author.

By evaluating the curves representing IP-Resistivity observed in the field together (Figures 7), an overall upward trend in resistivity behavior is initially apparent. The resistivity values corresponding to the shallowest layers (AB/2 up to 5m) show significant variations due to local variations in lithological components, primarily clay content and water presence. In particular, the surveys conducted in the landfill area (VES 02, 03, 05, 06), an area subject to constant surface alteration, exhibited the lowest apparent resistivity values for the layers.

In VES 02, 03, 04, 05, 06 (Figure 7), the resistivity behavior from the surface to a depth corresponding to an AB/2 spacing of 20m exhibits a geo-electric signature characteristic of sediments of the same nature. In this section, variations of up to 500 **Ω**·m occur, possibly related to saturation or local variations in clay content and porosity. Regarding these surveys, it was observed that there is little variation in resistivity, as well as induced polarization, naturally due to the surveys being located in the same area.

For AB/2 spacings greater than 20m, in these aforementioned surveys, a change in the concavity of the resistivity curve is observed, a significant reduction that is likely related to the static water level, i.e., the transition from the unsaturated zone to the saturated zone. In this context as well, induced polarization data show increasing values, confirming the suggested hypothesis.

As we reach the maximum AB/2 spacing, most of the surveys exhibit a descending behavior in resistivity values. This phenomenon may be related to sandy-clayey levels, which are very common in a fluvio-deltaic sedimentation environment, such as the São Sebastião Formation.

Figure 8: Geoelectric model.

Sector	Vertical Electrical Sounding	Physical Properties of Rocks	Layers					Geophysical Geological Model	
			1	2	3	4	5	Static Level	Interface Marizal S.Sebastião
Sector West	SEV02	Thickness (m)	2,22	9,5	3,77	85,8		11,7	15,5
		$\rho(\Omega.m)$	81,6	2102	131	585	41,5		
		M(mV/V)	1,51	3,22	2,19	4,43	15		
	SEV03	Espessura(m)	1,25	9,02	6,47	64,8		10,3	16,7
		$\rho(\Omega.m)$	62,8	1727	111	762	68,9		
		M(mV/V)	6,7	0,01	10,4	1,67	25,8		
	SEV05	Espessura(m)	2,78	8,86	3,36	15		11,6	15
		$\rho(\Omega.m)$	80,6	1908	320	524	219		
		M(mV/V)	9,86	0,01	0,01	8,76	4,84		
	SEV06	Espessura(m)	0,575	10,4	6,64	63,7		11	17,6
		$\rho(\Omega.m)$	169	406	231	966	836		
		M(mV/V)	2,14	2,14	8,02	0,261	7,11		
Sector East	SEVCP20	Espessura(m)	1,47	7,53	6,2	48,5		9	15,2
		$\rho(\Omega.m)$	1624	876	173	644	293		
		M(mV/V)	2,37	2,71	12,1	5,38	4,26		
	SEVCP18	Espessura(m)	1,46	7,93	16.09	63,7		9,38	26,3
		$\rho(\Omega.m)$	1513	4119	506	1728	564		
		M(mV/V)	2,27	0,572	12,03	8,53	0,01		
	SEVCP17	Espessura(m)	0,646	9,15	10.6	32,4		9,8	20,4
		$\rho(\Omega.m)$	577	1090	556	120	529		
		M(mV/V)	4,69	2,74	4,81	6,69	0,168		
	SEVCP16	Espessura(m)	0,907	10,7	6,9	42,4		11,6	18,5
		$\rho(\Omega.m)$	179	660	469	783	279		
		M(mV/V)	1,91	0,132	2,13	2,08	1,5		

Source: Created by the author.

The geoelectric model was subsequently compared with geophysical logging data and also with the well for water supply executed at an establishment adjacent to the landfill, more specifically within the Continental Tires factory domains. The distribution of resistivity values in depth shows a satisfactory correspondence with the Gamma and Electrical Resistivity data directly measured in the soil and rock. The position of the static water level is consistent with the values identified in the geophysical boreholes, with minor discrepancies associated with the fact that the geological profile was constructed during a different climatic period than when the SEVs were conducted (Figure 9).

Figure 9: Geophysical Data from the Investigative Well (PP24/03) and Geological Data from the Water Well (PMM-144/02).

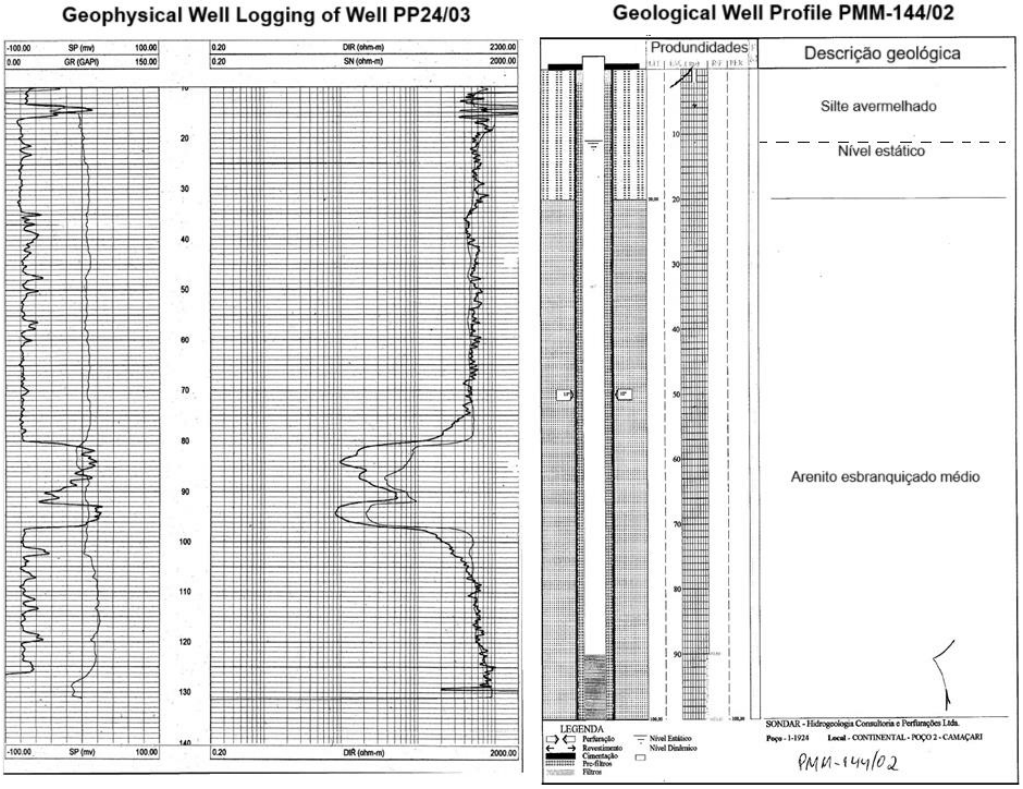

Source: Data provided by CETREL S.A. Company.

Figure 8 presents the final geo-electric models for the one-dimensional inversion of the apparent electrical resistivity curves shown in Figures 9 and 10. In these curves, the fourth layer generally exhibits high resistivity values, bounded by a more conductive layer. This geo-electric context allows us to infer that lithologically, this interval is related to fine sandstones, which make up the top of the São Sebastião Formation and are saturated with freshwater, at least throughout the extent of the investigated area.

Figure 9: SEV 01 interpreted.

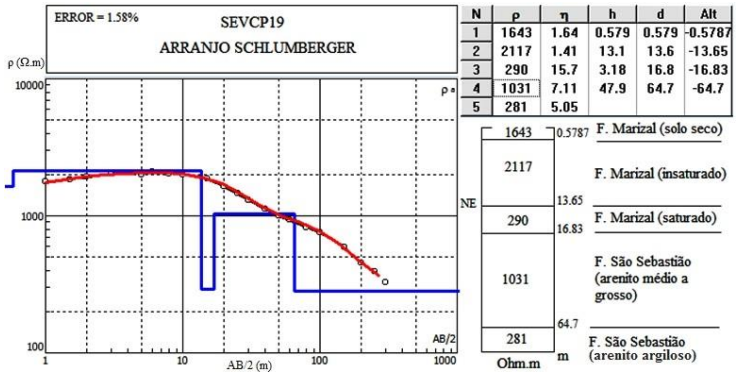

N	ρ	η	h	d	Alt
1	1643	1.64	0.579	0.579	-0.5787
2	2117	1.41	13.1	13.6	-13.65
3	290	15.7	3.18	16.8	-16.83
4	1031	7.11	47.9	64.7	-64.7
5	281	5.05			

Source: Created by the author.

VES surveys CP19 and VES04 (Figures 8 and 10) were conducted near wells PP 24/03 and PMM - 144/02. Their geological and geophysical profiles are in Annex II. This was done to obtain a standard IP-Resistivity model for the studied area, considering the appropriate local variations. In both images, we have an inverted resistivity curve shown in red, representing the actual resistivity behavior at a specific point on the surface. The vertical axis represents the resistivity scale (Ω·m), while the horizontal axis represents the current electrode spacing AB/2 (m). The straight-line segments in blue represent the layers, with thickness on the horizontal axis and resistivity on the vertical axis. The table alongside provides the inversion results: the N column represents the layer, the ρ (Ω·m) column contains the corresponding resistivity for each layer, n

represents induced polarization, h represents layer thickness, and d and Alt are parameters related to depth. Below this table is the interpreted geological model of the area with resistivity and depth values.

Figure 10: SEV 04 interpreted.

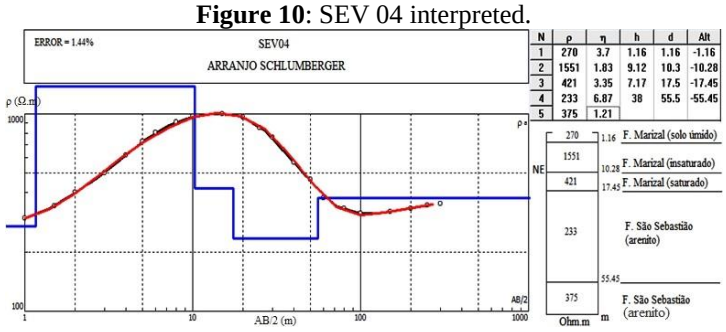

Source: Created by the author.

In both surveys, we can infer the presence of two electrically distinct substrates (unsaturated and saturated), followed by a resistivity contrast characteristic of lithological change from sandy-clayey to sandy, possibly the Marizal Formation/São Sebastião Formation interface. The last substrate obtained from the inversion is the most conductive and is interpreted as sandy-clayey in nature.

Figure 11 represents the geo-electric sections L01 and L02, both located within the landfill. Section L01 consists of VES CP10, CP11, CP12, CP13, CP14, CP15, and section L02 consists of VES 05, 03, 02. In this area, a resistivity pattern characteristic of sandy-clayey material for the initial AB/2 spacings up to 5m is observed, indicated in yellow in the figure. As observed in other VES surveys, this layer has a small thickness, with average values of 15m. In the domains corresponding to the maximum electrode spacing, most of the surveys show apparent resistivity values suggesting the presence of a highly resistive substrate. The high resistivity values found in the lower domain of this section, mainly in VES CP10, CP11, CP12, and CP13, may be associated with the presence of more compacted sandstones. From the middle to the lower part of section L01, the surveys provide indications of a slight tilt of the geo-electric layer and suggest saturation levels in all constituent surveys.

Figura 11: Geoelectric section L01.

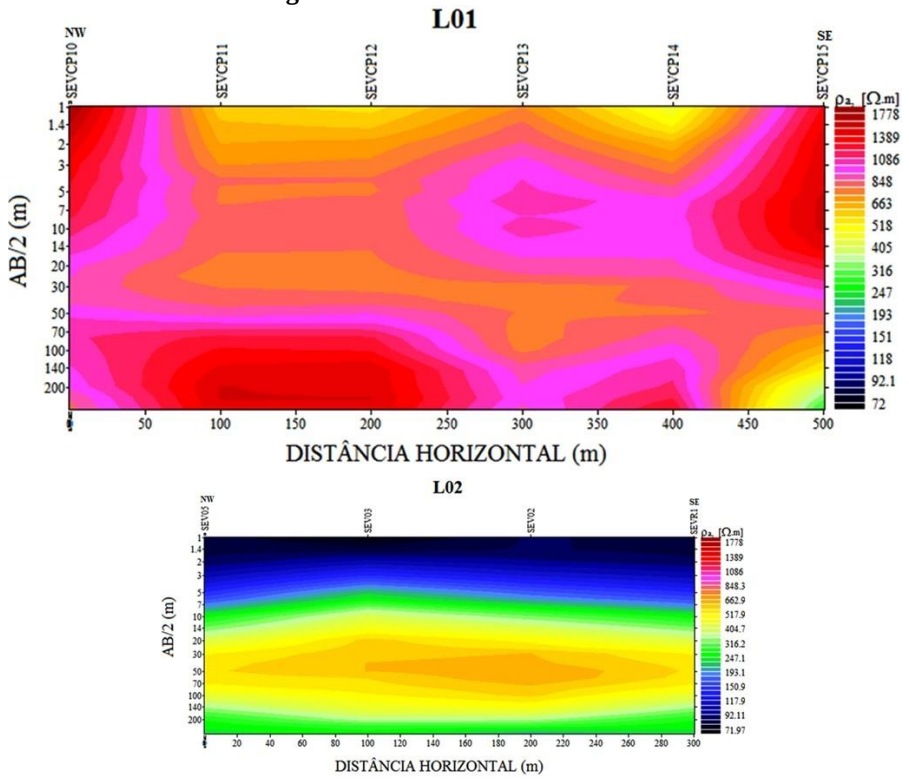

Source: Created by the author.

The surveys that make up sections L01 and L02, Figures 11 respectively, were conducted in the same section of the road but at different times. This section is where debris is constantly deposited, representing an area of constant alteration. Depending on the geo-electric nature of the deposited material, there will or will not be a change in the penetrability of electric current. These pieces of information explain the lack of satisfactory correspondence between resistivity values for the shallowest layers in both geo-electric sections.

In the same perspective as the geo-electric sections, this study used resistivity maps to analyze the geo-electric behavior of formations, both laterally and vertically. It also provided an overview of the predominant resistivity values in the region at shallow, medium, and deep levels. The idea of making a comparative analysis between resistivity maps for different AB/2 spacings in a sedimentary environment is to qualitatively identify the clay content in the studied area as well as aquifer zones (MOTA, 2004).

Figures 3.10 and 3.11 represent the resistivity behavior at a depth of approximately 5m (AB/2 of 10m). In most of the area, resistivity values are above 700 Ω·m, with variations from 50 Ω·m to 3,062 Ω·m. The high values identified at this investigation level are related to the unsaturated layers of the Marizal Formation. The peculiarity of this map is located in the landfill area, in more detail in Figure 3.11, where low resistivity values (up to 8.4 Ω·m) were recorded, which contrast with high IP values. The reason for such values is likely related to the production of leachate, a conductive material produced with the accumulation of solid waste. This material, in turn, migrates to deeper layers relatively easily, thus altering the resistivity of the percolated layers.

Figure 12: Contour map of apparent resistivity for the AB/2 electrode spacing at 10 meters.

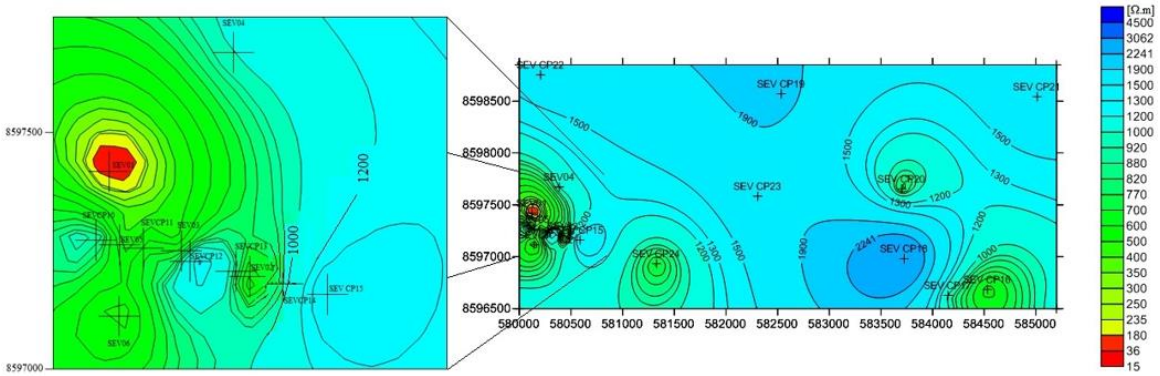

Source: Created by the author.

Figure 13: Contour map of apparent resistivity for the AB/2 electrode spacing at 10 meters.

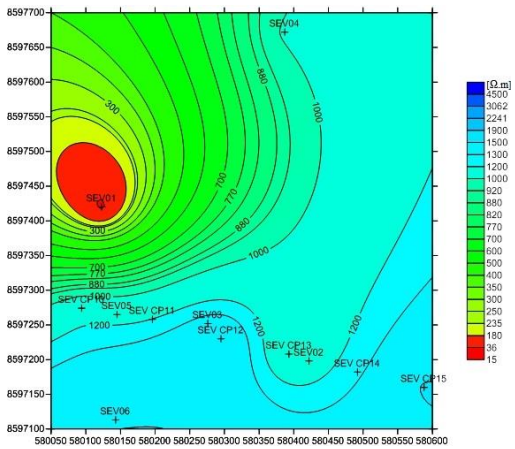

Source: Created by the author.

For the substrate corresponding to the AB/2 electrode spacing of 30m (Figures 14 and 15), most of the resistivity values range from 500 Ω·m to 1,500 Ω·m. The significant induced polarization effect presented at this investigation level, in the presence of moderate resistivity values, indicates the existence of sand-clay sediments saturated with water.

Figure 14: Contour map of apparent resistivity for the AB/2 electrode spacing at 30 meters

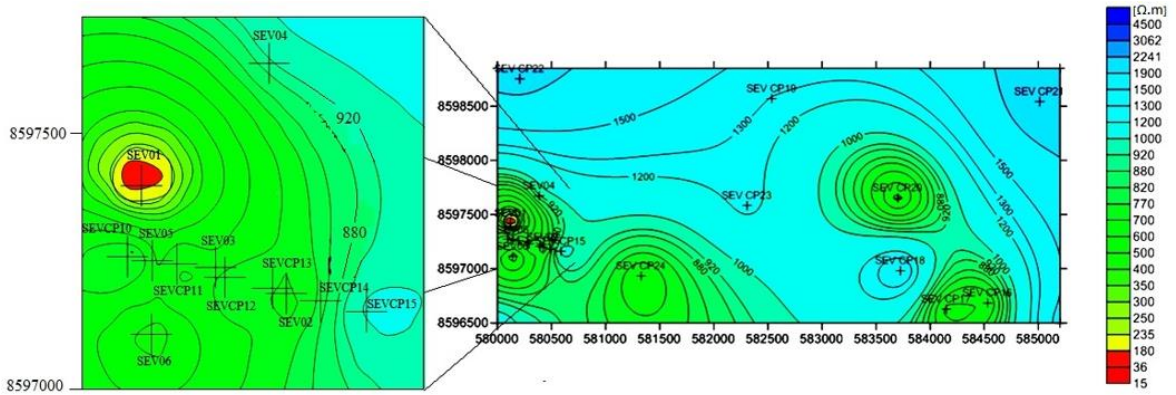

Source: Created by the author.

Figure 15: Contour map of apparent resistivity for the AB/2 electrode spacing at 30 meters in landfill area.

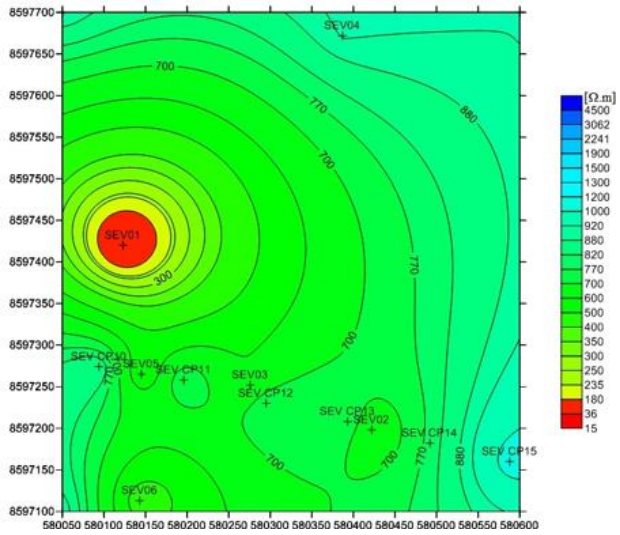

Source: Created by the author.

The resistivity data for the 300m electrode spacing, as shown in Figures 16 and 17, represents the deepest substrate investigated. Here, resistivity values range from 190 Ω.m to 4500 Ω.m, with average values of 1200 Ω.m. Overall, similar to what was observed in the geo-electric section L01 (Figure 11), the resistivity and chargeability values for this level of investigation indicate the presence of freshwater-saturated sandstones from the São Sebastião Formation. The variation in resistivity values observed at this investigation level may be related to variations in porosity in the study area, as well as the detection of clay layers.

Figure 16: Contour map of apparent resistivity for the AB/2 electrode spacing at 300 meters.

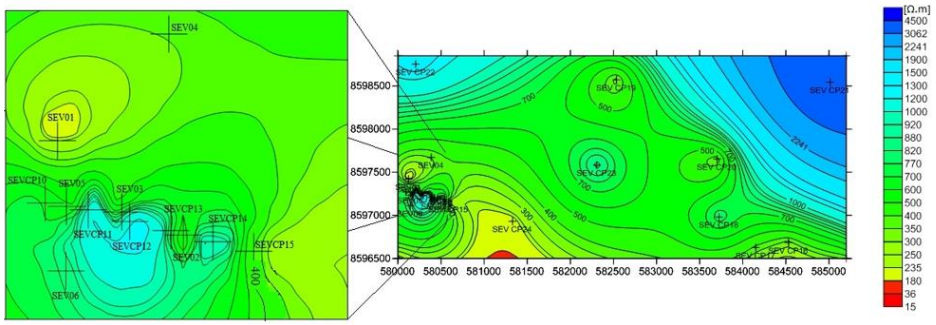

Source: Created by the author.

Figure 17: Contour map of apparent resistivity for the AB/2 electrode spacing at 300 meters in landfill area.

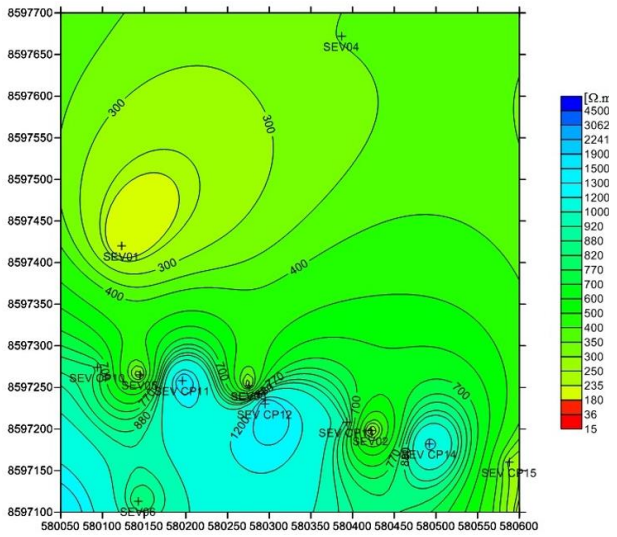

Source: Created by the author.

The construction of the final geo-electric profile (Figure 3.16) has a NW-SE orientation and is composed of the interpretation of one-dimensional inversions of the SEVs that make up the L01 and L02 lines (Figure 3.9). These SEVs include CP10, 05, CP11, 03, CP12, CP13, 02, CP14, CP15, positioned along a dirt road within the landfill area. In this profile, we can find the static water level (blue line), the geo-electric substrate representing the unsaturated zone (in green), the section representing the saturated Marizal Formation, and, at greater depths, the São Sebastião Formation, which is divided into two parts in the investigated area, one shallower and characterized as sandy (light blue), and another deeper part with a likely presence of sandy-clayey layers (dark blue)

Figure 18: Section formed by the one-dimensional inversions of the SEVs from lines L01 and L02.

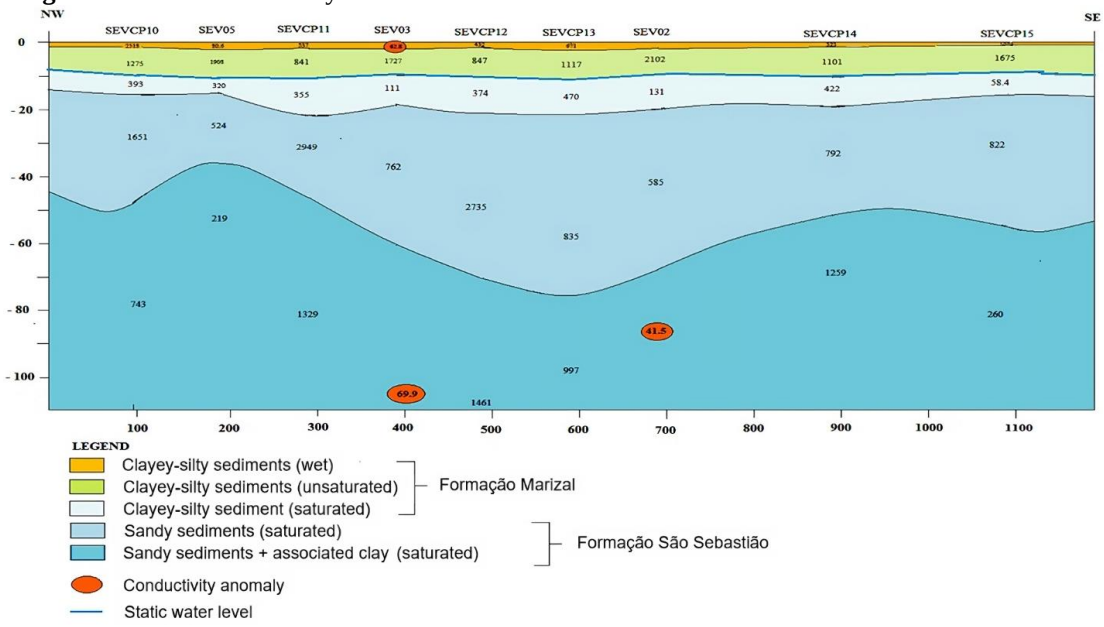

Source: Created by the author.

IV. Discussion

In the apparent resistivity and chargeability curves of Figures 3.5 and 3.6, conducted inside and outside the landfill, respectively, there are apparent resistivity and chargeability values that diverge for the initial spacings, AB/2 up to 5m. This is partly due to changes in the geo-electrical properties of the shallower layers due to landfill activities. With the increase in AB/2 spacing, in most of the SEVs, the apparent resistivity data from both figures tend to converge.

The unsaturated zone is evident in a significant portion of the boreholes, appearing as a highly resistive substrate due to little or no suspended water. This fact is also justified by the low values of induced polarization detected in the substrate. In many of the observed data, the static water level can be perceived when the ascending curve style gives way to a change in concavity with the increase in AB/2 spacing.

Through resistivity maps (Figures 3.10, 3.11, 3.12, 3.13, 3.14, 3.15), we can visualize three distinct domains. The domain corresponding to AB/2 spacing of 10m shows considerable variations in resistivity values. This difference is due to local variations in clay content, as well as the presence of suspended water. SEV01 is an exception, constituting an anomaly caused by continuous solid waste deposition. The depth domain corresponding to AB/2 spacing of 30m identified saturation levels in the Marizal Formation. At AB/2 spacing of 300m, we identified the aquifer of the São Sebastião Formation, represented by a highly resistive substrate with low chargeability values.

The final geo-electrical model defined the Marizal Formation with a depth of up to 27m in the studied area, with an average value of 15m. For the static water level, the average value is 10.5m, in agreement with local geological reality. The correlation established with well profiles (geological and geophysical) played a fundamental role in hydrogeological characterization, providing precise layer thicknesses and depths of aquifer horizons.

The depth of investigation in the boreholes varied considerably due to local differences in clay levels in the Marizal Formation, causing the maximum depths reached in the boreholes to vary in the same proportion. It was possible to identify the São Sebastião Formation with a layer of freshwater-saturated sand followed by a conductive layer, as in SEV CP24. The high resistivity values obtained for the deeper layers suggest that the eastern sector of the investigated area has lower porosities compared to the western sector.

One other factor to consider regarding the differences in resistivity values between sections L01 and L02 is the possible advancement of contaminants in depth. The migration of these contaminants can occur through the porous medium in a mechanism known as hydrodynamic dispersion (Bear, 1972).

V. Conclusion

The IP-Resistivity method proved to be efficient in the hydrogeological characterization of the study area by securely identifying typical hydrogeological features. Field geology corresponded satisfactorily to the established geoelectric model, with the exception of SEV01, which was conducted in the solid waste deposition area.

The distribution of resistivity values in the study area, both laterally and in depth, attests to the fact that landfill activities directly influence the degree of preservation of shallow groundwater, even though landfill operational protocols are being followed.

The methodological strategy adopted was able to efficiently identify and distinguish areas associated with soil contamination at the shallowest depths in the central area of the landfill. The ability to identify plumes of contamination and also verify the integrity of the soil sealing blankets attests to the efficiency of the method adopted for landfill management.

From an environmental perspective, geophysics contributes satisfactorily to the preservation of subsurface water resources, as it has the necessary tools to monitor the degree of human activity influence on the upper layers over time. Therefore, geophysics represents a new paradigm through which future generations will use to preserve available natural resources, accumulating information that will serve as a reference for more advanced studies.

Acknowledgement

I would like to thank the Research Center for Geology and Geophysics (CPGG) at the Federal University of Bahia for providing the infrastructure. I would also like to express my gratitude to Geophysicist Roberto Tiago Sobrinho da Silva for the operational support during the geophysical data collection.

References

[1]. Aragão, M A N F, Peraro A (1994) Elementos Estruturais do Rifte Tucano/Jatobá, In: Simpósio sobre o Cretáceo do Brasil, 3., Universidade Estadual Paulista, Boletim, Rio Claro-SP.
[2]. Archie G E (1942) The electrical resistivity log as an aid in determining some reservoir characteristics, Petroleum Transactions of AIME, n. 146: 5462.
[3]. Bear J (1972) Dynamics of fluids in porous media, American Elsevier Publishing Company, New York.

[4]. Bobachev A, Modin I N, Shevnin V (2000) IPI2WIN, Moscow State University and Geoscan-M. Ltd., Moscou.
[5]. Braga A C O (2006) Métodos da Eletrorresistividade e Polarização Induzida Aplicados nos Estudos da Captação e Contaminação de Águas Subterrâneas: uma Abordagem Metodológica e Prática, Tese (livre docência), Universidade Estadual Paulista, Rio Claro-SP, Brasil.
[6]. Brito I M., Mello C, Madeira C (2006) Avaliação do Significado Estratigráfico do Termo Barreiras, Anais da Academia Brasileira de Ciências, Brasil.
[7]. CNPS (2006) Sistema Brasileiro de Classificação de Solos, Embrapa, 2° ed., Brasília-DF.
[8]. Feitosa F A C, Manoel Filho J (2000) Hidrogeologia: conceitos e aplicacões, CPRM, 2.ED, Fortaleza.
[9]. Fonseca P P (2004) Mapeamento Geológico e Zoneamento Geoambiental da Região do Polo Industrial de Camaçari, através do uso de Ortofotos Digitais, Trabalho final de graduação, Universidade Federal da Bahia, Salvador-BA, Brasil.
[10]. Freitas F D S (2008) Modelagem Geoelétrica de Reservatórios em Ambientes de Águas Doces: Estudo de Sensibilidade de Medidas de IP-Resistividade na Exploração Petrolífera, Trabalho final de graduação, Universidade Federal da Bahia, Salvador-BA, Brasil.
[11]. Gabaglia G R e Milani E (1990) Origem e evolucão de Bacias sedimentares, Petrobras, Rio de Janeiro-RJ.
[12]. Ghignone J I (1984) Geologia dos Sedimentos Fanerozóicos do Estado da Bahia, In: Geologia e Recursos Minerais do Estado da Bahia, Textos Básicos, SME/CPM, 1.
[13]. Kirsch R, Yaramanci U (2006) Geophysical characterisation of aquifers, Groundwater Geophysics, Springer, Germany.
[14]. Lima O A L (1991) Reconstrução Arquitetural da Formação Marizal (Cretáceo Inferior) na Bacia do Recôncavo, Tese de Mestrado, Universidade Federal da Bahia, Salvador-BA, Brasil.
[15]. Lima O A L (1999) Caracterização Hidraúlica e Padrões de Poluição no Aquífero Recôncavo na Região de Camaçari-Dias D'ávila, Tese de concurso para professor titular, Universidade Federal da Bahia, Salvador-BA, Brasil.
[16]. Magnavita L P, Silva R S, Sanches C P (2005) Roteiros Geológicos, Guia de Campo da Bacia do Recôncavo, NE do Brasil, Petrobras, Boletim de Geociências, Rio de Janeiro-RJ.
[17]. Martins W O (2000) Inversão Conjunta de Dados de Eletrorresistividade e Polarização Induzida, Trabalho final de graduação, Universidade Federal da Bahia, Salvador-BA, Brasil.
[18]. Menke W (1984) Geophysical data analysis, Discrete inverse theory., Academic Press.
[19]. Milhomem P, Maman E, Oliveira F, Carvalho M, Sousa-Lima W (2003) Bacias Sedimetares Brasileiras, Bacia do Recôncavo., Fundação Paleontológica Phoenix, Revista Phoenix (on line), ano 5, Março, n.5, Rio de Janeiro-RJ.
[20]. Mota S U S (2004) Caracterização do Setor Oriental do Pólo Industrial de Camaçari Utilizando Geofísica Elétrica, Tese de Mestrado, Universidade Federal da Bahia, Salvador-BA, Brasil.
[21]. Silva O, Caixeta J, Kosin M. (2007) Bacia do Recôncavo., Petrobras, Boletim de Geociências, v.15(2), 423-431, Rio de Janeiro-RJ.
[22]. Szatmari P, Conceição J, Lana M, Milani E, Lobo A (1984) Mecanismo tectônico do riftamento sul-atlântico, In: Congresso Brasileiro de Geologia, Anais, v. 4, p. 1589-1601, SBG, Rio de Janeiro-RJ, Brasil.
[23]. Telford W M, Geldart L P, Sheriff R E (1990) Applied Geophysics, Cambridge University Press, London.
[24]. Viana C, Gama E J, Simões I, Moura J, Fonseca J, Alves R (1971) Revisão Estratigráfica da Bacia do Recôncavo/Tucano., Petrobras, Boletim de Geociências, v.14, 157-192, Rio de Janeiro-RJ.
[25]. Ward S (1990) Resistivity and Induced Polarization Methods., Geotechnical and Environmental Geophysics, Vol. 1, SEG, 147-189.
[26]. Warming (1981) Folha SD24 Salvador, geologia, geomorfologia, solos, vegetação, uso potencial da terra., Projeto Radam Brasil, Rio de Janeiro-RJ.
[27]. Waterloo (2003) Zoneamento dos Recursos Hídricos Subterrâneos na Região do Pólo Petroquímico de Camaçari/BA, Relatório Interno, CETREL Empresa de Proteção Ambiental, Camaçari-BA.